

γ -ray spectroscopy of odd-odd ^{62}Cu

B. Mukherjee, S. Muralithar, R. P. Singh, R. Kumar, K. Rani, and R. K. Bhowmik
 Nuclear Science Centre, Aruna Asaf Ali Marg, Post Box 10502, New Delhi 67, India

(Received 4 September 2000; published 20 April 2001)

Excited states of the odd-odd ^{62}Cu isotope were populated and studied via the ^{16}O (65 MeV) + ^{52}Cr reaction using a gamma detector array equipped with a charged-particle detector array for reaction channel separation. On the basis of γ - γ coincidence relations and angular distribution ratios, an extended level scheme was constructed up to $E_x = 10.88$ MeV and $J^\pi = (14^+) \hbar$, and $(14^-) \hbar$, and this result was interpreted in terms of shell model calculations with a restricted basis of the $f_{5/2}$, $p_{3/2}$, $p_{1/2}$, and $g_{9/2}$ orbitals outside a ^{56}Ni core.

DOI: 10.1103/PhysRevC.63.057302

PACS number(s): 23.20.Lv, 23.20.En, 21.60.Cs, 27.50.+e

The generation of higher spin states in the $A \sim 60$ region requires either a breaking of the ^{56}Ni core and/or excitation into the positive parity $g_{9/2}$ shell. The identification of this competing mechanism is one of the main motivations behind this study. The neutron deficient, odd-odd $^{62}\text{Cu}_{33}$ has been studied by several experimental techniques such as heavy-ion fusion-evaporation reactions [1,2], ϵ decay and transfer reactions such as those in Refs. [3–5]. These studies identified states in ^{62}Cu up to $E_x = 7.6$ MeV and $J^\pi = (12) \hbar$. The most recent heavy-ion fusion-evaporation reaction study of this nucleus was that of Singh *et al.* [2], who identified 70 γ rays in ^{62}Cu , of which one was placed ambiguously and as many as 20 were not placed in the level scheme due to the lack of proper coincidence requirement. Due to the weak population of this nucleus, Singh *et al.* were unable to determine the directional correlation orientation (DCO) ratios for many of the observed decays.

Here we report on the observation of 34 new γ rays and 21 unreported states, and a determination of DCO ratios for many of the γ rays associated with this nucleus. Spherical shell model calculations have been performed, and we found that these calculations adequately describe the observed high-spin states in ^{62}Cu .

High-spin states in ^{62}Cu were populated using the fusion evaporation reaction $^{52}\text{Cr}(^{16}\text{O}, \alpha pn)^{62}\text{Cu}$ at 65 MeV of beam energy, provided by the 15UD Pelletron accelerator of the Nuclear Science Centre (NSC). A 1-mg/cm² thin natural (85% abundance) target layer of ^{52}Cr was evaporated onto a 7.2-mg/cm² gold support foil. Prompt γ rays were detected using the Gamma Detector Array (GDA) (with a total photopeak efficiency of $\sim 0.5\%$ only) [6] of 12 Compton-suppressed germanium detectors (HPGe), in coincidence with the evaporated lightly charged particles to provide reaction channel selection. The charged particles were detected in the 4π Charged-Particle Detector Array (CPDA) [7], which comprises 14 $\Delta E - E$ phoswich plastic scintillating (BC400 and BC444) detectors. A total of 9.4×10^7 particle- γ events were collected in four days of beam time.

Altogether some six nuclei were produced, with measurable cross sections in this fusion reaction. Among them, the strongest channel, $^{62}\text{Cu} + \alpha pn$, comprises nearly one-third of the total fusion cross section. The γ - γ coincidence relationships for ^{62}Cu were derived from a $4k \times 4k$ matrix gated on the $1\alpha 1p$ channel. A representative γ spectrum of ^{62}Cu ,

shown in Fig. 1, is obtained by putting separate gates on 350-, 925-, and 980-keV transitions of a most intense yrast γ cascade, and summing them together. Coincidence, intensity balance, and summed energy relations were inspected to deduce the high-spin excitation scheme. The γ -ray energies and intensities presented in the level scheme are based on the $1\alpha 1p$ gated γ - γ spectrum matrix. But for weak transitions and/or doublet structures, γ -gated spectra obtained from total γ - γ matrix were considered. Spin and parity assignments were made on the basis of a DCO-type analysis [8] and from the known 1^+ spin-parity value of the ground state. A separate γ - γ coincidence matrix was constructed with events detected in detectors at 144° (θ_1) versus those at 99° (θ_2) detectors. By gating a transition of known multipolarity on each axis of the matrix, a DCO ratio

$$R_{\text{DCO}} = \frac{I_{\gamma_1}(\theta_1) \text{ gated by } \gamma_2(\theta_2)}{I_{\gamma_1}(\theta_2) \text{ gated by } \gamma_2(\theta_1)}$$

could be obtained. For an $(E2, E2)$ coincidence, R_{DCO} was found to be approximately 1.25, while for $(E2, E1/M1)$ pairs, $R_{\text{DCO}} \approx 0.62$. Pure nonstretched dipole ($L=1$, $\Delta J=0$) transitions are also expected to have R_{DCO} close to

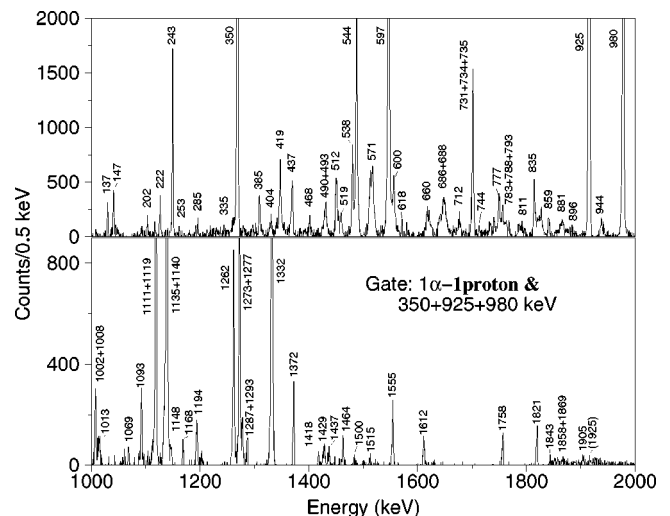


FIG. 1. γ - γ coincidence spectrum for ^{62}Cu gated on $1\alpha 1p$ and the transitions 350, 925, and 980 keV, highlighting the representative transitions of this nucleus.

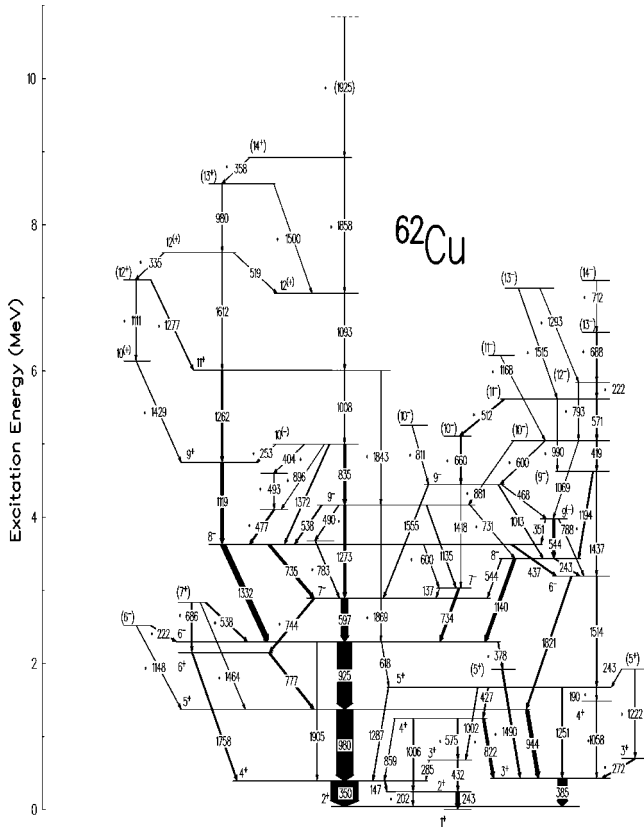


FIG. 2. Proposed level scheme for ^{62}Cu . All transitions have satisfied γ - γ coincidence conditions, and the width of the arrows corresponds to the relative γ -ray intensities. Newly placed transitions are marked by an asterisk.

unity. Definite parities were assigned to the excited states if one of their deexciting transitions was a stretched $E2$ or mixed $M1/E2$ transition, while in the case of pure dipole transitions only tentative parities were ascribed.

The level scheme of this nucleus, as determined in this experiment, is presented in Fig. 2, while representative spectra can be seen from Fig. 1. Tentative spin and/or parity assignments are indicated within parentheses. Unlike the low cross section of the reaction studied by Singh *et al.* [2], this nucleus was populated with a much higher fraction of total fusion cross section, making spectroscopy of this nucleus much easier. The level scheme presented in Fig. 2 is almost similar to that of Ref. [2] up to a moderate spin. Table I summarizes the results of this work. The identification and placement of the 519-keV transition is confirmed here. The DCO ratio measurements here are in good agreement with the tentative assignments made in Ref. [2].

Notable differences between this work and the work of Singh *et al.* [2] are as follows. (a) The 222-, 358-, 404-, 493-keV transitions, observed but unplaced due to lack of proper identification in Ref. [2], have been determined to form a part of the level scheme. On the other hand, the 606- and 681-keV transitions mentioned in above reference could not be observed at all in our study. (b) The 202-, 272-, 378-, 688-, 859-, 881-, 1058-, 1464-, and 1490-keV transitions, observed and identified but not placed in the level scheme in Ref. [2], due to the lack of statistics and proper coincidence

requirement, have been properly placed in the level scheme. But the 439-, 587-, 668-, and 1729-keV transitions, referred to in that paper, could not be observed in our study. (c) Compared with what was determined by Singh *et al.*, a total of 21 previously unreported states and 34 newly observed γ transitions have been properly placed, thereby extending the level-scheme of ^{62}Cu up to an excitation energy of ~ 10.88 MeV. We have observed some γ transitions viz. 202, 575, 600, 731, 744, 788, 881, 990, 1002, 1843, and 1869 keV, linking some already established levels. It should be mentioned here that three transitions at 788, 1437, and 1869 keV, decaying from 3977-, 4627-, and 4165-keV levels, respectively, happen to be $M3$ -type multipoles, although the spin-parity assignments of first two levels are tentative in nature.

Spherical shell model calculations were performed for ^{62}Cu , with a model space basis restricted to the $f_{5/2}$, $p_{3/2}$, $p_{1/2}$, and $g_{9/2}$ orbitals (henceforth called fpg shell calculations), using the OXBASH code [9]. The two-body matrix elements were taken from the work of Koops and Glaudemans [10]. The model assumes a closed ^{56}Ni core, and does not allow for core breaking. For both protons and neutrons, the single-particle energies of these active orbitals were calculated relative to the lowest $f_{5/2}$ state, and found to be 1.01 MeV for the $p_{3/2}$ orbital, 2.83 MeV for the $p_{1/2}$ orbital, and 0.68 MeV for the $g_{9/2}$ orbital.

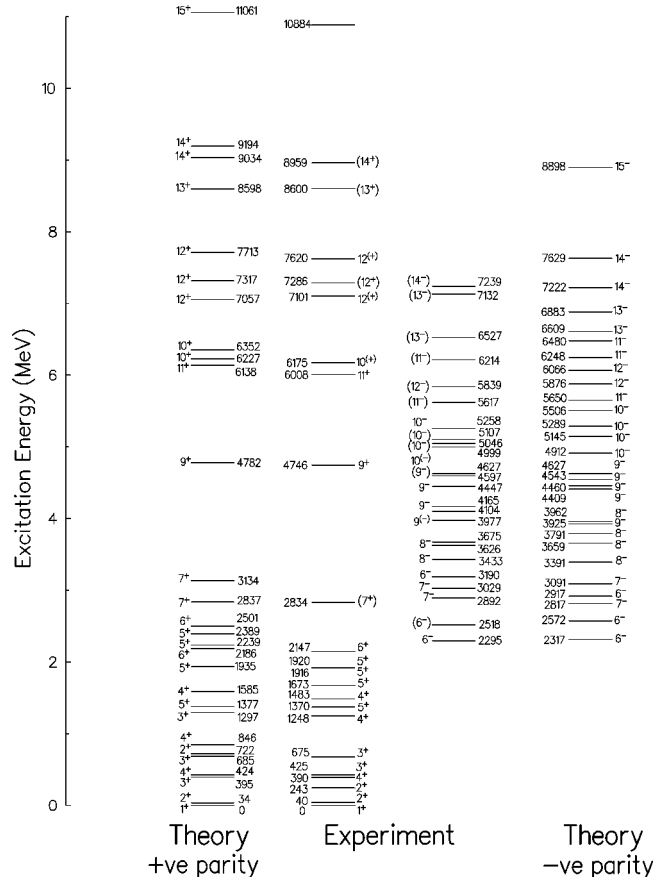


FIG. 3. A comparison of experimental data and fpg -shell model calculations for ^{62}Cu . The highly nonyrast calculated levels are not shown.

TABLE I. Level energies (E_x), transition energies (E_γ), initial (I_i^π) and final (I_f^π) spin parities of the transitions, relative intensities of γ -ray transitions (I_γ) and DCO ratios (R_{DCO}) are shown for ^{62}Cu . Level energies and transition energies are given to the nearest keV.

E_x (keV)	E_γ (keV)	I_i^π (\hbar)	I_f^π (\hbar)	I_γ (%)	R_{DCO}	E_x (keV)	E_γ (keV)	I_i^π (\hbar)	I_f^π (\hbar)	I_γ (%)	R_{DCO}
40						4104 ^a	477 ^a		8 ⁻	4.2±0.7	
243	202 ^a	2 ⁺	2 ⁺	2.1±0.6		4165	490 ^a	9 ⁻	8 ⁻	1.1±0.5	
	243	2 ⁺	1 ⁺	12.3±1.0	b		538	9 ⁻	8 ⁻	3.1±1.2	b
390	147	4 ⁺	2 ⁺	3.4±0.9	0.76±0.2 ^c		731 ^a	9 ⁻	8 ⁻	1.1±0.5	
	350	4 ⁺	2 ⁺	100.0±0.3	1.17±0.1 ^c		1135	9 ⁻	7 ⁻	2.4±1.0	0.96±0.2 ^d
425	385	3 ⁺	2 ⁺	35.2±0.4	0.51±0.1 ^c		1273	9 ⁻	7 ⁻	15.2±0.4	1.18±0.1 ^d
675	285	3 ⁺	4 ⁺	1.3±0.9	1.43±0.3 ^d		1869 ^a	9 ⁻	6 ⁻	1.1±0.7	
	432	3 ⁺	2 ⁺	3.7±1.2	1.67±0.1 ^e	4447	468	9 ⁻	9 ⁽⁻⁾	1.2±1.0	0.62±0.2 ^d
698 ^a	272 ^a	3 ⁺	3 ⁺	2.8±0.3	0.90±0.2 ^f		1013	9 ⁻	8 ⁻	2.0±0.4	0.45±0.3 ^d
1248	575 ^a	4 ⁺	3 ⁺	4.4±0.7			1418	9 ⁻	7 ⁻	1.0±0.7	
	822	4 ⁺	3 ⁺	9.2±1.0	1.18±0.2 ^f		1555	9 ⁻	7 ⁻	2.3±0.8	1.02±0.3 ^d
	859	4 ⁺	4 ⁺	1.2±0.7		4597 ^a	493 ^a			2.2±0.8	
	1006	4 ⁺	2 ⁺	3.0±0.7		4627	1194	(9 ⁻)	8 ⁻	4.1±0.8	1.87±0.3 ^d
1370	944	5 ⁺	3 ⁺	12.7±0.4	0.36±0.1 ^f		1437	(9 ⁻)	6 ⁻	1.2±0.8	
	980	5 ⁺	4 ⁺	61.8±0.3	3.80±0.1 ^d	4746	1119	9 ⁺	8 ⁻	9.5±0.5	2.42±0.1 ^d
1483 ^a	1058 ^a	4 ⁺	3 ⁺	1.2±0.5		4999	253 ^a	10 ⁽⁻⁾	9 ⁺	1.3±1.0	
1673	190 ^a	5 ⁺	4 ⁺	1.0±0.6			404 ^a	10 ⁽⁻⁾		1.0±0.3	
	427	5 ⁺	4 ⁺	3.3±1.2	0.71±0.4 ^f		835	10 ⁽⁻⁾	9 ⁻	9.4±0.4	1.61±0.2 ^d
	1002 ^a	5 ⁺	3 ⁺	2.0±0.3			896 ^a	10 ⁽⁻⁾		0.3±0.3	
	1251	5 ⁺	3 ⁺	4.5±1.4	1.43±0.5 ^f		1372	10 ⁽⁻⁾	8 ⁻	3.1±0.5	1.35±0.2 ^d
	1287	5 ⁺	4 ⁺	2.6±0.3	1.53±0.4 ^d	5046	419	(10 ⁻)	(9 ⁻)	3.0±0.7	0.56±0.3 ^d
1916 ^a	1490 ^a	(5 ⁺)	3 ⁺	5.3±0.3	0.89±0.3 ^c		600 ^a	(10 ⁻)	9 ⁻	1.5±0.7	
1920 ^a	243	(5 ⁺)	5 ⁺	1.0±0.8	b		881 ^a	(10 ⁻)	9 ⁻	0.9±0.5	
	1222 ^a	(5 ⁺)	3 ⁺	2.1±0.3	0.40±0.2 ^f		1069	(10 ⁻)	9 ⁽⁻⁾	0.8±0.7	
2147	777	6 ⁺	5 ⁺	3.4±0.8	0.58±0.3 ^d	5107 ^a	660 ^a	(10 ⁻)	9 ⁻	3.1±1.0	0.47±0.3 ^d
	1758	6 ⁺	4 ⁺	4.5±0.8	1.05±0.4 ^d	5258 ^a	811 ^a	(10 ⁻)	9 ⁻	1.0±0.3	0.51±0.2 ^d
2295	378 ^a	6 ⁻	(5 ⁺)	2.7±0.3	0.54±0.3 ^c	5617	512 ^a	(11 ⁻)	(10 ⁻)	3.3±0.8	0.67±0.3 ^d
	618	6 ⁻	5 ⁺	1.4±0.5			571	(11 ⁻)	(10 ⁻)	4.2±0.6	0.68±0.2 ^d
	925	6 ⁻	5 ⁺	53.6±0.3	1.52±0.1 ^d		990 ^a	(11 ⁻)	(9 ⁻)	1.0±0.4	
	1905	6 ⁻	4 ⁺	1.0±0.7		5839 ^a	222 ^a	(12 ⁻)	(11 ⁻)	2.2±0.3	0.58±0.3 ^d
2518 ^a	222 ^a	(6 ⁻)	6 ⁻	1.0±0.4			793 ^a	(12 ⁻)	(10 ⁻)	1.3±0.7	
	1148 ^a	(6 ⁻)	5 ⁺	1.3±0.3	1.20±0.5 ^d	6008	1008	11 ⁺	10 ⁽⁻⁾	3.2±1.0	0.88±0.2 ^d
2834 ^a	538 ^a	(7 ⁺)	6 ⁻	3.2±0.6	b		1262	11 ⁺	9 ⁺	6.0±0.6	1.23±0.1 ^d
	686 ^a	(7 ⁺)	6 ⁺	3.3±0.7	0.58±0.3 ^d		1843 ^a	11 ⁺	9 ⁻	0.3±0.3	
	1464 ^a	(7 ⁺)	5 ⁺	1.3±0.4	1.12±0.4 ^d	6175 ^a	1429 ^a	10 ⁽⁺⁾	9 ⁺	1.7±0.3	0.61±0.3 ^d
2892	597	7 ⁻	6 ⁻	24.2±0.4	2.46±0.1 ^d	6214 ^a	1168 ^a	(11 ⁻)	(10 ⁻)	1.0±0.3	0.49±0.3 ^d
	744 ^a	7 ⁻	6 ⁺	4.5±0.3		6527 ^a	688 ^a	(13 ⁻)	(12 ⁻)	1.3±0.4	0.45±0.3 ^d
3029	137	7 ⁻	7 ⁻	1.5±0.8	0.78±0.4 ^d	7101	1093	12 ⁽⁺⁾	11 ⁺	1.6±0.7	2.02±0.3 ^d
	734	7 ⁻	6 ⁻	7.6±0.4	b	7132 ^a	1293 ^a	(13 ⁻)	(12 ⁻)	1.0±0.6	
3190	1514	6 ⁻	5 ⁺	1.2±0.7			1515 ^a	(13 ⁻)	(11 ⁻)	1.1±0.7	1.05±0.5 ^d
	1821	6 ⁻	5 ⁺	2.3±1.0	2.87±0.5 ^d	7239 ^a	712 ^a	(14 ⁻)	(13 ⁻)	0.5±0.3	
3433	243	8 ⁻	6 ⁻	2.3±1.1	b	7286 ^a	1111 ^a	(12 ⁺)	10 ⁽⁺⁾	0.9±0.3	
	544	8 ⁻	7 ⁻	2.3±0.7			1277 ^a	(12 ⁺)	11 ⁺	2.1±0.4	0.59±0.3 ^d
	1140	8 ⁻	6 ⁻	10.2±1.0	1.78±0.1 ^d	7620	335 ^a	12 ⁽⁺⁾	(12 ⁺)	1.0±0.8	
3626	437	8 ⁻	6 ⁻	3.5±0.8	1.32±0.2 ^d		519	12 ⁽⁺⁾	12 ⁽⁺⁾	1.5±0.5	0.47±0.3 ^d
	600 ^a	8 ⁻	7 ⁻	1.5±0.6			1612	12 ⁽⁺⁾	11 ⁺	1.5±0.7	0.62±0.3 ^d
	735	8 ⁻	7 ⁻	7.2±0.3	b	8600 ^a	980	(13 ⁺)	12 ⁽⁺⁾	1.0±0.8	
	1332	8 ⁻	6 ⁻	16.4±0.4	1.33±0.1 ^d		1500 ^a	(13 ⁺)	12 ⁽⁺⁾	1.0±0.7	
3675 ^a	783 ^a		7 ⁻	2.3±1.0		8959 ^a	358 ^a	(14 ⁺)	(13 ⁺)	0.5±0.5	
3977	351	9 ⁽⁻⁾	8 ⁻	2.0±1.2			1858 ^a	(14 ⁺)	12 ⁽⁺⁾	1.0±0.7	1.87±0.6 ^d
	544	9 ⁽⁻⁾	8 ⁻	10.3±1.2	2.40±0.2 ^d	(10884) ^a	(1925)		(14 ⁺)	0.5±0.5	
	788 ^a	9 ⁽⁻⁾	6 ⁻	1.5±0.5							

^aEnergy level/ γ ray, either not reported or not placed earlier.

^bCould not be measured because of overlap with the doublet partner.

^cE2 gating transition: 1332 keV.

^dE2 gating transition: 350 keV.

^eM1 gating transition: 243 keV.

^fM1 gating transition: 385 keV.

For ${}^{62}_{29}\text{Cu}_{33}$, the *fp*g-shell model space has five valence neutrons and one valence proton in the four active orbitals, and the maximum angular momentum that can be generated is $(\pi g_{9/2})^1_{9/2^+} \otimes (\nu g_{9/2})^4_{12^+} \otimes (\nu f_{5/2})^1_{5/2^-} = 19^- \hbar$. Guided by the transfer data, we restricted the configuration in $k \leq 5$ with the $(0f_{5/2}, 1p_{3/2}, 1p_{1/2})^{A-56-k} (0g_{9/2})^k$ model space. The results of this calculation are compared with the experimental levels in Fig. 3. It is noted that the coupling is weak among different k ($k=0, 1, 2, 3, 4$, and 5) configurations in the calculated result. The calculation reproduces the yrast states quite well in the whole region under investigation. For all the yrast states the energy spacing, level density, and level ordering are correctly predicted. We do see a crossing of level sequences with different configurations. The energy increases with J are slower for the higher configuration, which is obvious around the crossing region. The crossing structure accounts for the parity change in the experimental yrast sequences. The negative parity level becomes yrast at $J=6$.

In summary, the high-spin states of ${}^{62}\text{Cu}$ have been studied with the GDA+CPDA configuration, identifying previously unobserved states up to an excitation energy of 10.88

MeV. From the observed decays of states and DCO ratios, it was possible to assign spins and parities of many of the states observed. The resulting level scheme has been compared with shell model calculations, using a simple *fp*g basis. In general, reasonable agreement has been established between experimental results and simple *fp*g-shell model calculations, suggesting that the low-lying yrast excited states in this nucleus correspond predominantly to valence particle excitations into the $f_{5/2}$, $p_{3/2}$, and $p_{1/2}$ orbitals. Higher-energy and spin states are fairly well accounted for by allowing only excitations into the $+ve$ parity $g_{9/2}$ orbital, with no core breaking.

The authors would like to thank the operating crew of the Pelletron facility at Nuclear Science Centre. Special thanks are due to Dr. S. K. Datta, Dr. A. Roy, Dr. D. Kanjilal, Dr. T. Nandi, Prof. N. Singh (P.U.), Prof. S. C. Pancholi (D.U.), Dr. S. Ghugre (IUCDAEF), Dr. G. Mukherjee, Mr. D. Kabiraj, Mr. S. Chanda (VECC), and Mr. P. Barua for helpful discussion during and after the experiment. One of the authors (B.M.) gratefully acknowledges the research grant from the University Grants Commission (India).

-
- [1] T. U. Chan, M. Agard, J. F. Bruandet, A. Giorni, F. Glasser, J. P. Longequeue, and C. Morand, Nucl. Phys. **A293**, 207 (1977).
 [2] A. K. Singh *et al.*, Phys. Rev. C **59**, 2440 (1999).
 [3] K. Nilson, B. Erlandsson, and A. Marcinkowski, Nucl. Phys. **A391**, 61 (1982).
 [4] H. M. Sen Gupta, J. B. A. England, F. Khazaie, E. M. E. Eawas, and G. T. A. Squier, Nucl. Phys. **A517**, 82 (1990).
 [5] M. M. King, Nucl. Data Sheets **60**, 337 (1990).
 [6] S. C. Pancholi and R. K. Bhowmik, Indian J. Pure Appl. Phys. **27**, 660 (1989).
 [7] B. Mukherjee, S. Muralithar, R. P. Singh, R. Kumar, K. Rani, S. C. Pancholi, and R. K. Bhowmik, Pramana J. Phys. **55**, L471 (2000).
 [8] A. Kramer-Flecken, T. Morek, R. M. Lieder, W. Gart, G. Hebbinghaus, H. M. Jager, and W. Urban, Nucl. Instrum. Methods Phys. Res. A **275**, 333 (1989).
 [9] B. A. Brown, A. Etchegoyen, W. D. M. Rae, and N. S. Godwin (unpublished).
 [10] J. E. Koops and P. W. M. Glaudemans, Z. Phys. A **280**, 181 (1977).